



Special Issue of Second International Conference on Advances in Science Hub (ICASH 2021)

Forecasting Drought via Soft-Computation Multi-layer Perceptron Artificial Intelligence Model

Nivedika¹, Mahendra Meghwal², PV Ramana³

^{1,2,3}Department of Civil Engineering, Malaviya National Institute of Technology Jaipur, India.

pvrmana.ce@mnit.ac.in³

Abstract

Drought is a natural and gradual threat, with many devastating consequences for all aspects of human life. Accurate drought forecasting is a promising step to help decision-makers develop strategies to manage drought risks. To achieve this goal, choosing a suitable model plays a vital role in the forecasting method. Various artificial neural network (ANN) models are used to predict short-term and long-term droughts on different time scales using the Standardized Precipitation Index (SPI), including 3, 6, 12, 24, and 48 months in Rajasthan and Gujarat. Due to the frequent danger of drought, people today are facing many environmental challenges. It affects the environment of the country, community and industry. Some of the adverse effects of the drought threat persist in Pakistan, including other threats. However, early measurement and identification of drought can guide for water resources management to use drought-resistant strategies. In this article, we use the Multilayer Perceptron Neural Network (MLPNN) algorithm to predict drought. 17 weather stations in Daman and Diu.

Keywords: SPI, Precipitation, Groundwater, SDAT Models, Artificial Intelligence

1. Introduction

Drought refers to that period in a year where there is a scarcity of rainwater, leading to dry and hot weather. The term drought is complex. Drought can bring lots of physical change to the environment. It brings about significant effects on nature and the people. It has a long-lasting impact on Humans. Droughts are one of the deadliest natural calamities due to less rainfall. Drought is most harmful because agriculture is one of the primary sources in India, and it is dependent on rainfall and water supply; a shortage in water affects agriculture badly, resulting in Famine and Inflation and causes deaths on a large scale. Drought also affects the environment in many different ways. Plants and Animals depend on water, just like people. Lack of food and drinking water leads to an increase in disease in wild animals. Wild life's existence can also end if the species keep on dying because of drought. If they did not get enough water or food due to drought, it

would create an overall environmental problem. India's agriculture is largely dependent on the country's climate-the favourable southwest summer monsoon is essential to provide irrigation water for Indian plants. In parts of India, insufficient rainfall has led to water shortages, which has led to a decline in average production. Large areas of arid regions, such as southern and eastern Maharashtra, northern Karnataka, Andhra Pradesh, Orissa, Gujarat, Telangana and Rajasthan. Died; the famine of 1980-2012 caused more than 5 million deaths, and the famine of 1980 caused more than 4.5 million deaths. The drought of 1972 affected 2.5 million people in Maharashtra. In short, the drought destroyed India. All these severe droughts. The El Niño drought also led to a cyclical decline in agricultural production in India; however, the ENSO event coincided with India's unusually high sea surface temperature. Indian ocean. In one case in 1997 and 1998, ocean

evaporation rose to 3°C (5°F), resulting in unusually humid weather throughout India. This happened during the long warm period that began in the 1990s. On the contrary, unlike the usual high-pressure air masses, the oceanic low-pressure convergence centre connected to ENSO is forming over the southern Indian Ocean; during the humid summer monsoon, it continuously inhales dry air from Central Asia, and the changes that are taking place in India have dried up. This reverse air current is causing drought in India. Drought. In India, part of the El Niño phenomenon is accompanied by drought. Within the total geographical area of India, nearly one-sixth of the population accounts for 12% of drought-affected land; areas with an annual rainfall of up to 60 cm are at the greatest risk. The Irrigation Commission (1972) identified 67 drought-prone areas. This includes 326 Taluk, which is located in 8 states and covers 49.73 million hectares. The criteria for identifying some areas prone to drought are slightly different. After careful investigation, it was found that 74 areas outside the country were at risk of drought—Zeng Chaohao and so on. (2013) [4] Several indicators are used to monitor drought, such as the Standardized Precipitation Index (SPI), which is based on several indicator variables. Due to the complexity of the causes and effects of drought, a variable is used to monitor drought. It May is not sufficient to quickly and reliably determine drought conditions. MSDI), which describes drought as a function of precipitation and soil moisture. In this study, MSDI uses data from the United States Drought Monitoring Agency (USDM) and standardized indices commonly used to monitor droughts (including droughts). , And the geographic coverage of the continental United States. Alireza Farahmand, wait. Current performance is affected by defects such as time drift and statistical inconsistency. Most drought indicators are based on probability distribution functions of representative parameters that fit the data; however, parameter distribution functions may not provide any data, especially for continental/global studies. The non-parametric structure applied to various climate variables (including precipitation, soil moisture, and relative humidity) does not represent the parameters' representative distribution. Drought severity Step 1. Create an initial chromosome population. Step 2

Run the ANN model to predict the drought severity category and calculate its applicability. The most attractive feature of this scheme is that it results in a statistically consistent drought rate based on various variables. And others. (2020) [6], groundwater modelling has become a valuable tool to support political decision-makers to formulate effective/sustainable management strategies for this precious natural resource. [1-5].

2. Methodology:

This paper proposes an MSDI to characterize general drought conditions, considering insufficient precipitation and insufficient soil moisture. This method extends the SPI widely used by McKee et al. Taking the humidity on a certain time scale (such as 1 month or 6 months) as a random variable X or Y, the joint distribution of the two variables (X and Y) can be expressed as:

$$P(X \leq x, Y \leq y) = p \quad (1)$$

Where p represents the joint probability of precipitation and soil moisture, and MSDI can be defined as a function of the joint probability p (Hao and AghaKouchak 2013):

$$\text{MSDI} = \Phi^{-1}(p) \quad (2)$$

Where Φ is the standard normal distribution function. Like SPI, MSDI is derived from the (overall) probability of the variable of interest, which can be used to collect drought information on different time scales (such as 1, 3, usually expressed in equation (1). Built-in multi-parameter connection, it is necessary to carefully evaluate the parameters and fitting criteria to estimate the drought severity algorithm: one input layer, one or more hidden layers and one output layer of SPI3, it takes three months to calculate The window is the average correlation coefficient 0.90, Nuwara Eliya has the lowest 0.84, Batticaloa and Jaffna have the highest 0.94. In general, the forecast accuracy of stations in dry areas is higher than that of stations in wet areas. May to July (the first part of the southwest monsoon season) compared to the rest of the year. The accuracy of the prediction increases with the length of the window used to calculate the SPI value. It shows that the neural network model trained by SPI can be used to predict water shortage.

$$y_k(t) = f_0 \left[\sum_{j=1}^m w_{kj} \cdot f_n \left(\sum_{i=1}^N w_{ji} x_i(t) + (w_{j0}) + w_{k0} \right) \right] \quad (3)$$

Where N is the number of samples, m is the number of hidden neurons, $x_i(t)$ =input variable in

i^t ; w_{ji} = the weight of connecting the i -th neuron of the input layer and the j 'th neuron of the hidden layer; Another group of perfect hybrid models uses wave-based preprocessing techniques to decompose predictor variables or target indicators and then use independent or even hybrid machine learning methods to train them. Another variant.

3. Methodology & Problem Statement:

Rajasthan is prone to hunger and drought, especially in the westernmost part of the Thar Desert, which often experiences years of scarcity and scarcity. Atmospheric circulation leads to stable atmospheric subsidence. Recent studies on the interaction between global circulation and drought indicate that the El Niño Southern Oscillation (ENSO) phase has a major fault impact on India. For example, the lack of rain combined with the unpredictable behaviour of the state's monsoon makes Rajasthan the most vulnerable to drought. For example, some studies use artificial intelligence-based models to predict drought in different locations and under different conditions;

4. Results and discussion:

The total rainfall data collected from the India water portal used for the drought assessment. This data collected at all tehsil/sub-tehsil rain gauge stations of Rajasthan for the year 2016. With the help of rainfall data, the Average yearly rainfall has been calculated, shown in Fig.1, on the x-axis, there are several rain gauge stations of all districts of Rajasthan and on y-axis rainfall (mm). The figure below maximum rain took place in Baran district (46.4% more than average), minimum precipitation took place in Jaisalmer district (17.3% less than expected) in 2016. In Fig.2, on the x-axis, there is the number of rain gauge stations in all districts of Rajasthan, and on the y-axis, Drought occurrence is Probable. As a result, the highest probability was found for Jaisalmer district, and minimum probability was found for Baran, Pali, and Churu district.

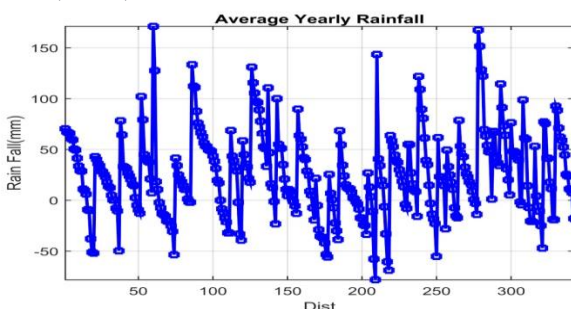


Fig. 1. Showing average yearly rainfall

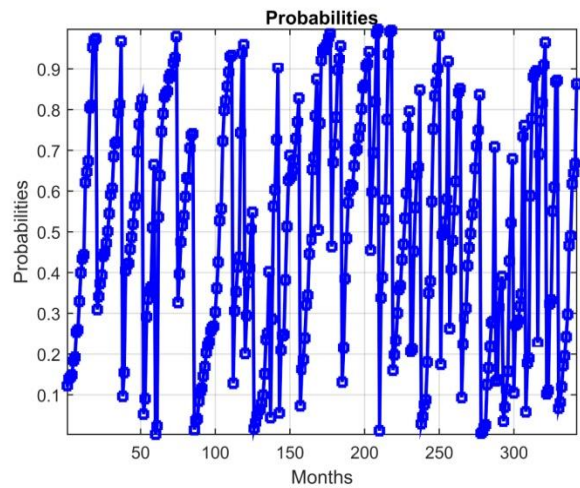


Fig. 2. Showing probability of drought occurrence

Similarly, in Fig.3, the probability of drought occurrence due to soil moisture for 6 months has been calculated, where q_n is soil moisture content and $q_n(1), q_n(2), \dots, q_n(6)$ showing Probability for May, June, ..., October. Here on the x-axis, there is the number of rain gauges of all districts of Rajasthan, and on the y-axis probability of drought occurrence due to soil moisture condition. $q_n(1)$ figure shows the probability of drought occurrence due to soil moisture condition for May month. The curve showing the maximum likelihood is for Alwar and Hanumangarh district, and the minimum is for Bharatpur, Bhilwara, Jhalawar, and Pali district. For $q_n(2)$, the same probability curve, the maximum likelihood (probability) is for Alwar and Hanumangarh district, and the lowest chance (probability) is for many communities such as Ajmer, Bharatpur, Sawai Madhopur, Tonk, and Udaipur. For $q_n(3)$, the same probability curve, the maximum likelihood is for the Hanumangarh district. The minimum probability is for many communities such as Ajmer, Bharatpur, Sawai Madhopur, Tonk, and Udaipur. Figure $q_n(4), q_n(5),$ and $q_n(6)$ are showing similar results for maximum and minimum probabilities.

In Fig.4, risk assessment done due to sensitivity of soil moisture for 6 months, where s_n is the sensitivity of soil moisture and $s_n(1), s_n(2), \dots, s_n(6)$ showing the Probability for May, June, ..., October. The x-axis in all the 6 figures shows the number of rain gauge stations, and the y-axis shows the probable sensitivity in soil moisture. From all the curves of Fig.4 it's concluded that maximum sensitivity was in May, and the minor sensitivity was in October.

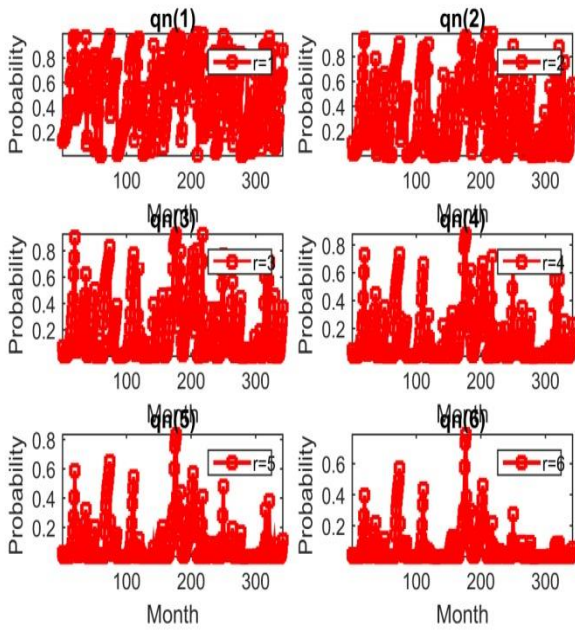


Fig. 3. Probability of drought due to soil moisture content for 6 months (May to October)

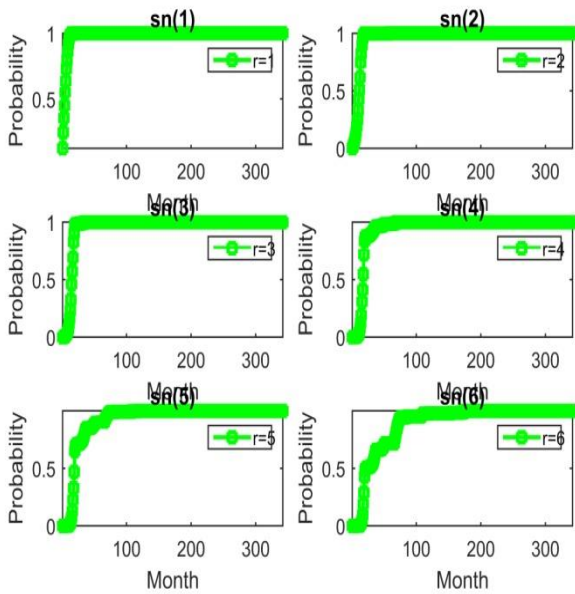


Fig. 4. Moisture Sensitivity for 6 months (May to October)

In Fig.5, the period of retention is shown. The minimum value is 7.6, and the maximum value is 9.8, which means the drought can occur once every year, 3 months (Minimum time), and once in one year, 7 months (maximum time). Fig.6, shows the standardized precipitation index (SPI) values with time at the x-axis and SPI on the y-axis. The maximum value of SPI is for Churu and Pratapgarh district. Minimum values were found for Dungarpur and Jaipur.

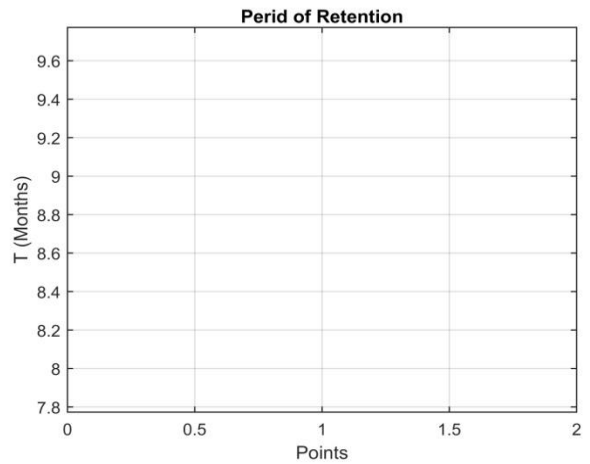


Fig. 5. The retention period for drought

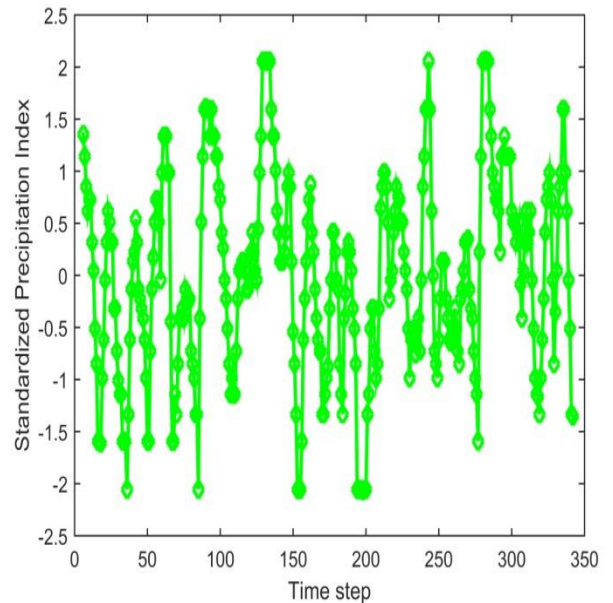


Fig. 6. Standardized precipitation index for Rajasthan in 2016 from SDAT

Figure 7 shows the calculated monthly precipitation data represents the generalized basis for obtaining univariate and multivariate non-parametric standardized indices. It can be seen that compared with other drought indexes, the proposed system provides the maximum frequency of drought events in the three sectors. It is recommended that the drought events reported by the system in the current period are usually classified according to the degree of drought, while other drought indices show inconsistencies. These figures show that the SPI curve has more fluctuations, and in SSI, there is minimal fluctuation which means that the SSI is similar at different places throughout the state. In the same way, variations of MSDIe and MSDIp can be seen

in the figures below. Fig.8, shows all the indices are all compared (SPI, SSI, MSDIe, MSDIp) for 6 months; the green curve shows the SPI, and the blue curve shows the SSI, the red curve is showing MSDIe, and the black curve is showing MSDIp. It's noted that MSDIe and MSDIp show almost the same results, while SPI showed significant variation compared to other indices.

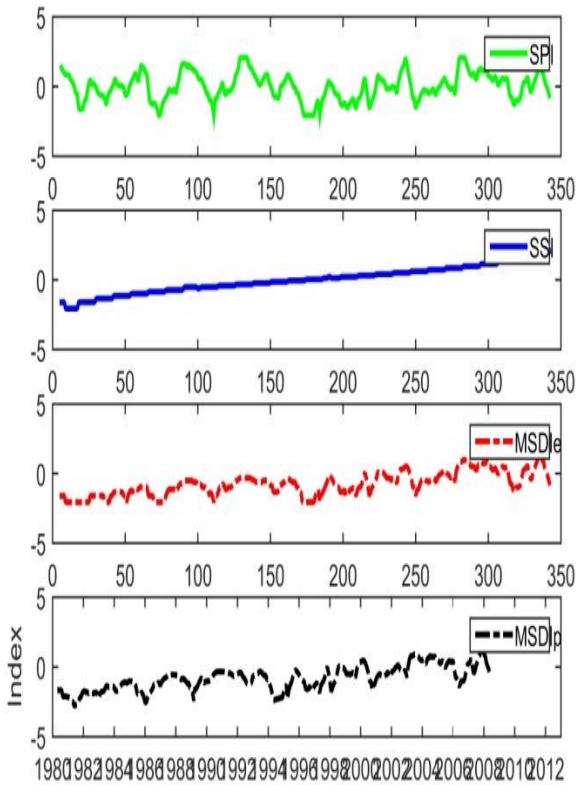


Fig. 7. SPI, SSI, MSDIe, MSDIp, respectively

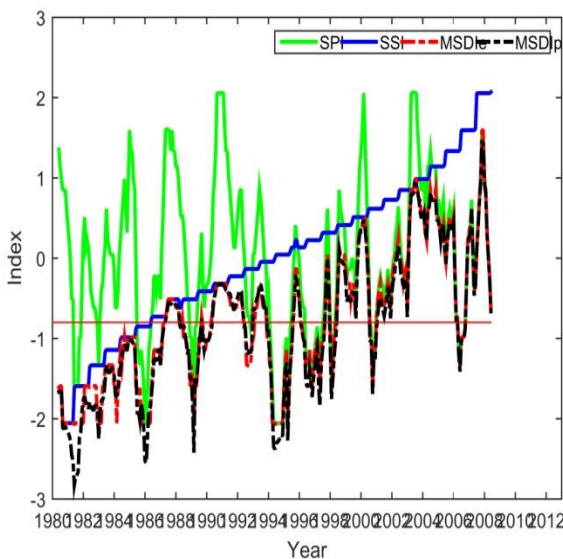


Fig. 8. Comparison of SPI, SSI, MSDIe, and MSDIp for 6 months

MSDIp 6 months For artificial intelligence (AI) development, optimizing model parameters to find the best configuration is critical. The best framework for AI drought prediction is that it has developed and thoroughly tested a mathematical algorithm. If consistent data and a sufficient number of neurons are available in its hidden layer, a two-stage feed network with hidden sigma neurons and linear output neurons can be suitable for multi-dimensional display tasks. The network is trained using the Levenberg-Marquardt propagation algorithm. As follows: Training (70%): The number of samples trained and presented in the network during the training process, and the network is adjusted and verified according to its error (15%): These data samples are used to measure the network and become better when generalization stops. Evidence of stop learning at the time (15%): They do not affect training and provide an independent evaluation of network perforation during and after training. The root means the square error is the mean square error between the result and the target. The lower the value, the better; zero means no errors. Figure 9 shows that the mean square error (MSE) peaks in 1000 periods. Fig. 10 shows the 3 levels of the training state diagram of the neural network (3101) with a combined structure of 3 input nodes, 10 hidden nodes, and 1 output node. If the credit check in each cycle reaches 0 credibility checks, the learning ends. The gradient descent value of 1000 is 0.04219, and the reasonable mu value is 0.001, which leads to rapid network convergence. For temperature, PDSI shows the maximum correlation value, and for groundwater, SPI12 shows the maximum correlation value for the best correlation.[6-12].

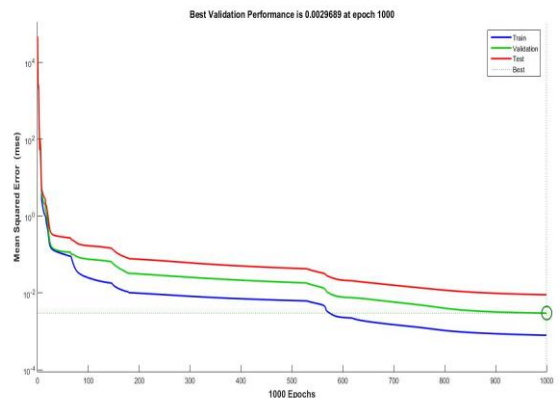


Fig. 9. Performance plot for the trained neural network

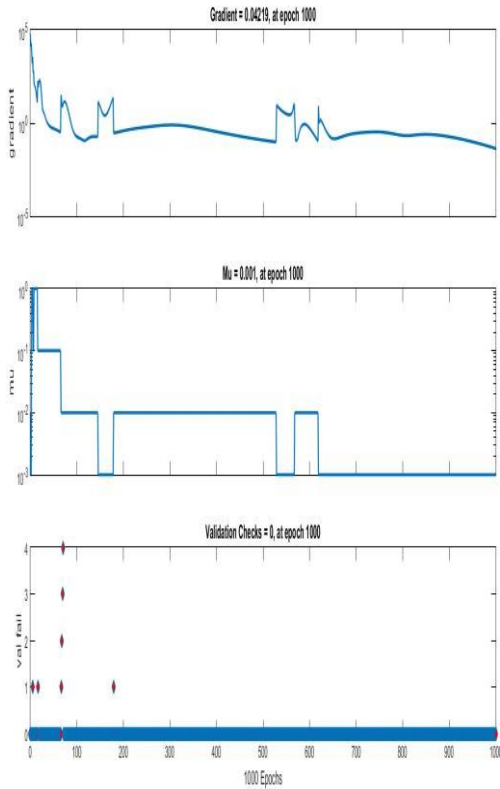


Fig. 10. Artificial Intelligence training state plot with 10 hidden nodes

The columns represent test data, and the red columns represent test data. The histogram can show outliers; H. The fit is significantly lower than most other data points. The r2 regression value measures the correlation between the result and the target. The value of r2 is 1 means the relationship is close, and 0 means the relationship is weak. In Figure 12, three graphs show training, validation, and test data. Expected result product = goal. The solid line represents the linear regression line that best meets the results and goals. The r2 value represents the relationship between the result and the target. If $r2 = 1$, it means that there is an exact linear value. The relationship between product and purpose. When r2 is close to zero, there is no linear relationship between the result and the target. Two types of translation functions. In the hidden structure of the AI layer. One transfer function is used between the input layer and the hidden layer, and the other is used between the hidden layer and the output layer. The most commonly used transfer functions are the Cleanliness transfer function, the tangential hyperbolic transfer function, and the logarithmic

transfer function. The proposed architecture uses protocol transfer functions (Logs) in the hidden layer and bandwidth transfer functions in the output layer. The value in the hidden neuron is given by Equation 1.[13-18].

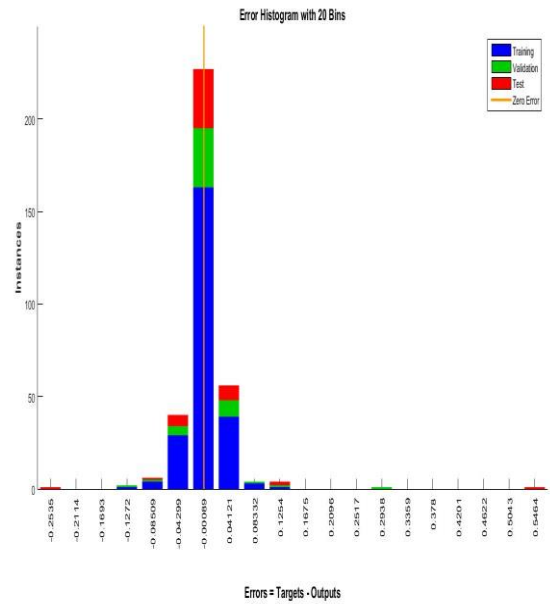


Fig. 11. Neural network error histogram

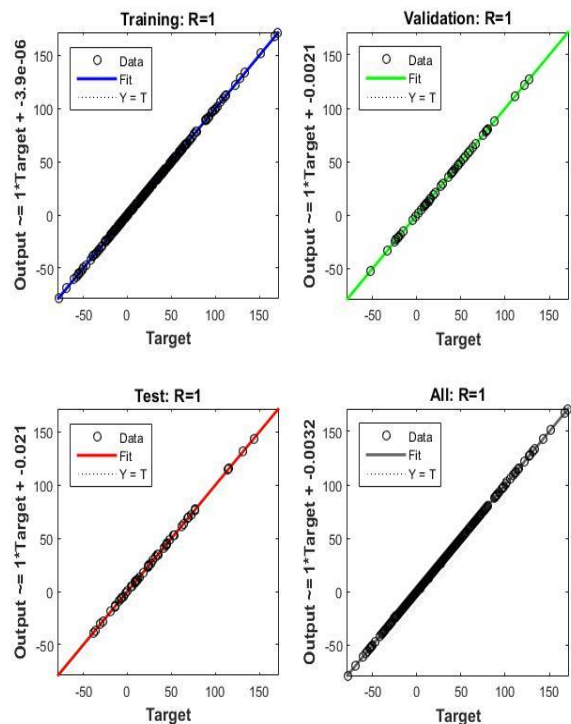


Fig. 12. Neural network regression curves for training, validation, and test data

Conclusions

In this study, artificial neural networks were used to predict short-term and long-term droughts in the Indian states of Rajasthan, Gujarat, Daman and Diu. In the first step, SPI is calculated on different time scales based on the precipitation time series. The forecast method uses several hydrometeorological variables, including precipitation, wind speed, sunshine hours, and humidity during the 22 years from 1980 to 2012. The SPI time series is predicted using the first two months of the above variables. They are developed based on different combinations of inputs and other architectures. Each model uses three indicators, namely CC, RMSE, and MAE.

References

- [1]. Anamika Agnihotri, Ajay Singh Jethoo, PV Ramana (2021), Mechanical and Durability Analysis of Recycled Materials, Key Engineering Materials (2021), ISSN: 1662-9795, Vol. 882, pp 228-236
- [2]. Ayush Meena, PV Ramana (2021), Impact of Blast Loading over Reinforced Concrete Structure Elsevier: Materials Today. <https://doi.org/10.1016/j.matpr.2021.04.139>
- [3]. PV Ramana, Arigela Surendranath, Anamika Agnihotri, & Kunal Bisht, (2021), "Functioning of bi-material interface intended for polypropylene fibre concrete", Materials Today: Proceedings, vol:38, pg:3397-3404
- [4]. Amir Aghakouchak, Zengchao Hao (2013), Multivariate Standardized Drought Index: A parametric multi-index model, Advances in water resources Elsevier journal, 57 (12- 18)
- [5]. Alireza Farahmand, Amir AghaKouchak, A generalized framework for deriving nonparametric standardized drought indicators, Advances in water resources Elsevier journal, 76 (140- 145)
- [6]. Janaki B Mohapatra, Piyush Jha, Madan K Jha, Sabinaya Biswal, Drought forecasting using new machine learning methods, Science of the total environment Elsevier, Vol. 785
- [7]. R. Alanis, A. Ingolfsson, B. Kolfal, A Markov chain model for an EMS system with repositioning, Prod. Oper. Manag. 22 (1) (2013) 216–231. W.S.S. Lam, Z.C. Zhang, H.C. Oh, Y.Y. Ng, W. Wah, ME Hock Ong, Reducing ambulance response times using discrete event simulation, Prehosp. Emerg. Care 18 (2) (2014) 207–216.
- [8]. Nivedika, PV Ramana (2021) Probabilistic Model to Predict the Fire Risk Incidental Duration, Elsevier Journal of Materials Today, 05, 2021, ISSN-2582-4376.
- [9]. Ramkesh Prajapat, PV Ramana Computational Intelligence on High Rise Structure with Effect of Diverse Load Conditions, Elsevier Journal of Materials Today, 05,2021, ISSN-2582-4376
- [10].Mahendra Meghwal, PV Ramana (2021), Soft Computation of Important Structures, Elsevier Journal of Materials Today, 05,2021, ISSN-2582-4376.
- [11].Anamika Agnihotri, Ajay Singh Jethoo, P.V. Ramana, Mechanical properties of unprotected recycled concrete to fiery-hot, Materials Today: Proceedings (2021), ISSN 2214-7853.
- [12].Surendranath, Arigela, and P. V. Ramana. (2021). "Recycled materials execution through digital image processing." Materials Today: Proceedings.
- [13].Ayush Meena, PV Ramana (2021)., Assessment of structural wall stiffness impact due to blast load Materials Today: Proceedings, Elsevier Publication.
- [14].Prateek Papriwal, Nivedika, (2021), "Influence of Vibration in High-Rise Building with Tuned Mass Damper Account into Diverse Loads", Elsevier Journal of Materials Today, 05, 2021, ISSN-2582-4376.
- [15].P V Ramana, Surendra nath, 2013, "A novel analysis for superstructures", Proceedings of current challenges in Structural Engineering, YRGS- 2013, India.
- [16].PV Ramana, Arigela Surendranath, Anamika Agnihotri, & Kunal Bisht, (2021), "Functioning of bi-material interface intended for polypropylene fibre concrete", Materials Today: Proceedings, vol:38, pg:3397-3404.
- [17].Md Masroor, Sufia Rehman, Ram Avtar, Meheeb Sahana, Raihan Ahmed, Haroon Sajjad (2020), Exploring climate variability and its impact on drought occurrence: Evidence from Godavari Middle sub-basin, India, Weather and Climate Extremes Elsevier journal 30 – 100277
- [18].Aishwarya Narang, International Conference on Advances in construction materials and structures (ACMS-2018) in IIT Roorkee.